

# Pressure-Driven Abnormal Emission Blue-Shift of Lead-Free Halide Double Perovskite $\text{Cs}_2\text{AgInCl}_6$ Nanocrystals

Ao Chen,<sup>||</sup> Xiaoling Jing,<sup>||</sup> Tianyuan Wang, Tingting Zhao, Yu Zhang, Donglei Zhou,<sup>\*</sup> Rui Sun, Xueting Zhang, Ran Liu, Bo Liu, Qunjun Li,<sup>\*</sup> and Bingbing Liu



Cite This: *Inorg. Chem.* 2022, 61, 6488–6492



Read Online

ACCESS |



Metrics & More

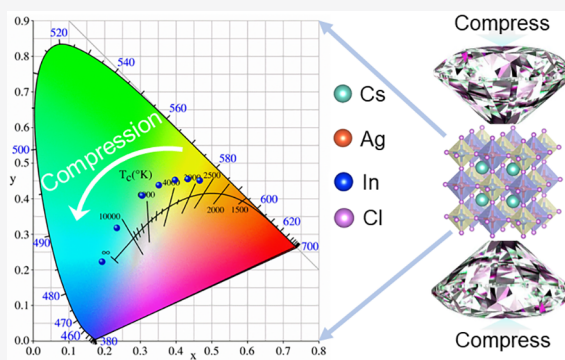


Article Recommendations



Supporting Information

**ABSTRACT:** Lead-free halide double perovskites (DPs) have been proposed as stable and promising alternatives to lead halide perovskites. Understanding the structural–optical properties of halide DPs is important for their applications. In this study,  $\text{Cs}_2\text{AgInCl}_6$  DP nanocrystals, with a direct band gap, were synthesized and studied. Because of a strong electron–phonon coupling leading to exciton self-trapping, a broad emission with a large Stokes shift of  $\text{Cs}_2\text{AgInCl}_6$  DP nanocrystals is observed. We observed an abnormal blue-shifted emission accompanied by a red-shifted direct absorption edge because of the reduced electron–phonon coupling under compression in the cubic phase  $\text{Cs}_2\text{AgInCl}_6$  DP nanocrystals. Our study clarified the basic structural–optical correlation of halide DPs and may promote their application in related fields.



## INTRODUCTION

Lead halide perovskites (LHPs) are extensively evaluated for use in solar cells, light-emitting diodes (LEDs), X-ray detectors, and scintillators,<sup>1–6</sup> owing to their special properties, such as their high carrier mobility derived from the “defect tolerant” structure.<sup>7–10</sup> Irrespective of the size, Pb-based perovskites typically exhibit inherent instabilities caused by exposure to moisture, oxygen, light, and heat.<sup>1–3</sup> Considerable effort has been spent to improve the inherent stability, such as ion doping,<sup>4</sup> changing the crystal structure,<sup>5,6</sup> decreasing the dimensionality, etc. Moreover, the toxicity of lead ions is also an obstacle to the commercialization and widespread use of LHPs.

To overcome these challenges, much effort has been spent to find environmentally friendly and stable halide perovskites.<sup>14–16</sup> For the substitution of Pb, several Pb-free perovskites have been discovered in the past few years.<sup>17,18</sup> Among these compounds, Bi- and Ag-based halide double perovskites (DPs) without Pb have been proposed and synthesized in recent years as stable and environmentally friendly alternatives.<sup>7,8</sup> However, these Bi- and Ag-based DPs show indirect band gaps. Indirect band gap materials are not suitable for thin-film photovoltaic applications, because an indirect band gap implies weak oscillations that cause optical absorption and radiative recombination.<sup>20</sup> To circumvent this limitation,  $\text{Cs}_2\text{InAgX}_6$  ( $X = \text{Cl}, \text{Br}, \text{or I}$ ) compounds, with direct band gaps corresponding to the spectral response range from the ultraviolet (UV; for  $X = \text{Cl}$ ) to the visible (for  $X = \text{I}$ ), were synthesized. The  $\text{Cs}_2\text{AgInCl}_6$  DP nanocrystals, with direct

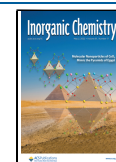
band gaps, are an ideal Pb-free alternative to the LHP nanocrystals.<sup>9</sup>

Recently, several excellent studies on improving the properties of DPs were performed. Li et al. optimized the synthesis parameters, such as preparing cubic  $\text{Cs}_2\text{AgInCl}_6$  DP nanocrystals with a narrow size distribution by adjusting the Cs:In:Ag:Cl precursor ratio. The obtained nanocrystals exhibited unique absorption and emission optical transitions. Additionally, doping significantly modified the optical and electric properties of the halide DP nanocrystals. The Yb- and Er co-doped  $\text{Cs}_2\text{AgInCl}_6$  DP nanocrystals retained their structural integrity and exhibited infrared emissions from their 4f orbital energy levels.<sup>10–12</sup>  $\text{Ho}^{3+}$ -doped  $\text{Cs}_2(\text{Na},\text{Ag})\text{-InCl}_6$  exhibited intense warm white emissions, as well as the characteristic emission of  $\text{Ho}^{3+}$  ions.<sup>13</sup>

As reported, high-pressure technology can be a clean tool for adjusting the lattice parameters and electronic configuration of materials and was used to change the various physical and chemical properties of materials without introducing impurities.<sup>14,15</sup> In recent years, conventional halide perovskites under compression have been widely studied, and various new phenomena have been reported, such as pressure-induced

Received: January 18, 2022

Published: April 15, 2022



amorphization,<sup>16</sup> metallization, band gap modulation,<sup>16,22</sup> and emission enhancement.<sup>20</sup> However, only a few studies of halide DPs under high pressure have been reported thus far.<sup>16,17</sup> Using high-pressure methods to explore the structure and properties of Cs<sub>2</sub>AgInCl<sub>6</sub> DP nanocrystals can aid in gaining an atom-level understanding for a fundamental study of such materials.

In this study, we evaluated the optical–structural properties of Cs<sub>2</sub>AgInCl<sub>6</sub> DP nanocrystals under an applied pressure at room temperature via in situ high-pressure photoluminescence (PL), absorption, and X-ray diffraction (XRD) techniques. Under the ambient conditions, the Cs<sub>2</sub>AgInCl<sub>6</sub> DP nanocrystals exhibited a direct band gap. We observed a broad emission peak with a large Stokes shift, as well as a negative shift in the emission peak relative to the absorption edge, caused by the decreased lattice relaxation energy under compression. No phase transition occurred during the pressurization. The results of this study reveal the structure–property relationships in halide DPs and enhance our fundamental understanding of them.

## RESULTS AND DISCUSSION

We employed an improved thermal injection method to synthesize the Cs<sub>2</sub>AgInCl<sub>6</sub> DP nanocrystals in this study.<sup>18</sup> Transmission electron microscopy (TEM) images indicate the uniform cubic morphology of the synthesized Cs<sub>2</sub>AgInCl<sub>6</sub> DP nanocrystals (Figure 1a). All of the crystals analyzed by high-

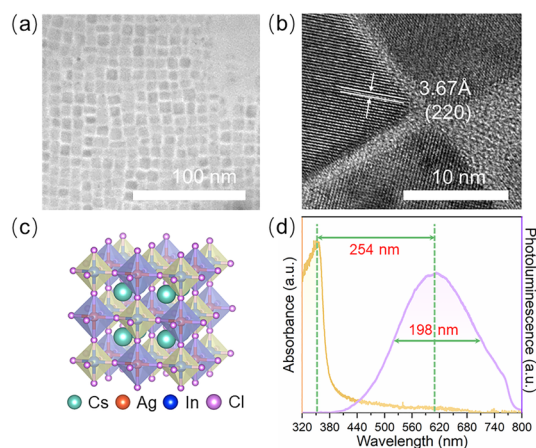


**Figure 1.** Characterization of the Cs<sub>2</sub>AgInCl<sub>6</sub> DP nanocrystals: (a) TEM image, (b) HRTEM image, (c) polyhedral model, and (d) absorption and PL spectra.

resolution TEM (HRTEM) had high crystallinity. The lattice fringe distances are determined to be 3.67 Å, which correspond to the known bulk lattice parameter of the (220) plane of the Cs<sub>2</sub>AgInCl<sub>6</sub> DP nanocrystals with a cubic phase (space group *Fm* $\bar{3}$ *m*) as shown in Figure 1b.<sup>19</sup> From the crystal structure diagram of Cs<sub>2</sub>AgInCl<sub>6</sub> (Figure 1c), we can see that the unit cell includes InCl<sub>6</sub> and AgCl<sub>6</sub> octahedra arranged in a face-centered cubic structure. An atomistic model includes InCl<sub>6</sub> and AgCl<sub>6</sub> octahedra alternating in three different orientations ([100], [010], and [001]). The absorption spectrum of the Cs<sub>2</sub>AgInCl<sub>6</sub> DP nanocrystals demonstrates an absorption edge located at  $\sim$ 360 nm. In addition, Cs<sub>2</sub>AgInCl<sub>6</sub> DP nanocrystals exhibit broad self-trapped exciton (STE) emission with a full width at half-maximum (fwhm) of 198 nm, which is consistent with the literature.<sup>9</sup> Furthermore, a large Stokes shift of 254

nm (Figure 1d), originating from the strong exciton–phonon coupling, was observed along with remarkable quantum effects.

To explore the photophysical properties of the Cs<sub>2</sub>AgInCl<sub>6</sub> DP nanocrystals at different pressures, in situ high-pressure PL and absorption spectroscopy measurements were performed. As shown in Figure 2a, under 360 nm UV radiation, the emission of Cs<sub>2</sub>AgInCl<sub>6</sub> DP nanocrystals is centered at approximately 609 nm, which is consistent with the previously reported results.<sup>21</sup> With an increase in pressure and a decrease in PL intensity, the PL peak evidently blue-shifts from 609 to 452.6 nm at 5.26 GPa and almost disappears at approximately 6.65 GPa. The PL intensity and peak position of the Cs<sub>2</sub>AgInCl<sub>6</sub> DP nanocrystals under the applied pressure are shown in panels b and c, respectively, of Figure 2. Moreover, the fwhm of the PL spectrum decreases remarkably upon compression (Figure S1). The observed shift of the PL peak toward higher energies is distinctly different from that observed in the studies of conventional Pb-based halide perovskites under high pressures. According to these previous studies, the blue-shift of the PL peak possibly occurs via a different mechanism under pressure, and this phenomenon could be repeated in our experiments. In addition, we recorded the CIE chromaticity coordinates under pressure of the PL emission by the Cs<sub>2</sub>AgInCl<sub>6</sub> DP nanocrystals, as shown in Figure 2d (details provided in Table S1). The CIE chromaticity coordinates change continuously from 0 GPa, (0.4656, 0.4522), to 5.26 GPa, (0.212, 0.22). The emission and absorption energies at different pressures were also recorded (Figure S2). Under ambient conditions, the Stokes shifts are ascribed to the strong coupling between excitons and the lattice.<sup>21</sup> Upon compression, the Stokes shift decreased remarkably, indicating a decrease in the electron–phonon coupling strength.<sup>20,21</sup> The emission peaks exhibited a quite large blue-shift upon compression, while the absorption peaks exhibited a slight red-shift that resulted in a gradual decrease in the Stokes shift. Thus, altering the emission intensity and chromaticity of halide DPs via high-pressure technologies is a progressive strategy, which can be used to optimize LED designs, with various chromaticities, for versatile applications in pressure engineering. The unusual blue-shifted emission of the Cs<sub>2</sub>AgInCl<sub>6</sub> DP nanocrystals inspired us to examine the changes in its band gap under a high pressure through in situ high-pressure absorption measurements. The pressure-dependent absorption spectra of the Cs<sub>2</sub>AgInCl<sub>6</sub> DP nanocrystals show a red-shift of the direct band gap from 0 to 5.81 GPa (Figure 2e). Then, a blue-shift of the absorption edge occurs, following a persistent blue-shift up to 12.6 GPa. With a further increase in the pressure, the steep absorbance weakens and leaves an absorption tail at pressures of  $>$ 16.6 GPa, which may be ascribed to pressure-induced amorphization. The band gap of the Cs<sub>2</sub>AgInCl<sub>6</sub> DP nanocrystals was assessed to be 3.37 eV under ambient conditions, consistent with that reported previously.<sup>9</sup> The band gaps of the Cs<sub>2</sub>AgInCl<sub>6</sub> DP nanocrystals were quantified from the Tauc plots of  $(\alpha d h\nu)^2$  versus  $h\nu$ , where  $\alpha$  is the absorption coefficient,  $h\nu$  is the photon energy, and  $d$  is the sample thickness.<sup>22</sup> The band gap value decreases until the applied pressure equals 5.81 GPa and then increases (Figure 2f). As observed in a few reported studies, perovskites exhibit an abnormal blue-shifted emission along with a red-shift of the absorption edge. On the basis of the results of our study, feasible methods for modulating and adjusting the optoelectronic transport characteristic of halide DPs can be developed.

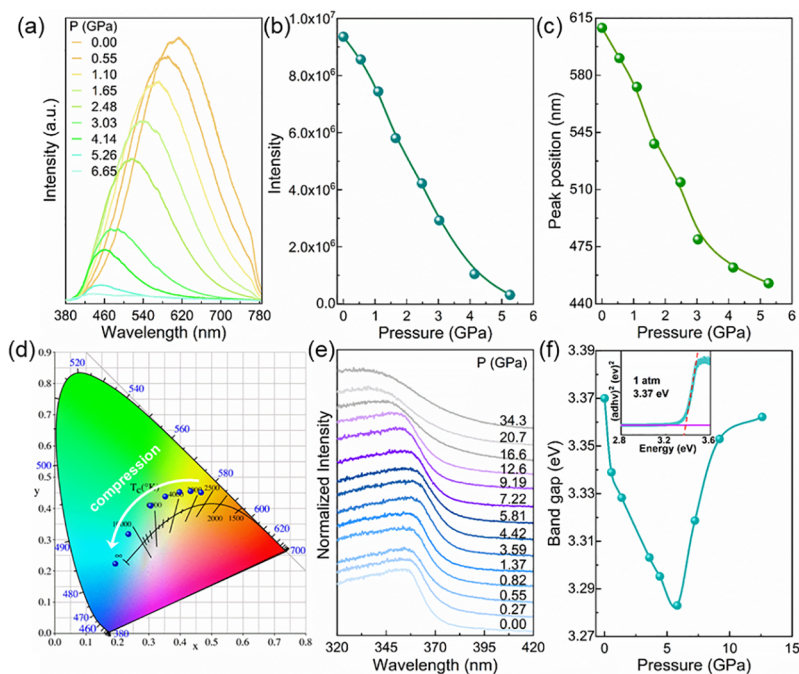


**Figure 2.** (a) Pressure-dependent PL spectra of the  $\text{Cs}_2\text{AgInCl}_6$  DP nanocrystals. (b) PL intensity and (c) position of the  $\text{Cs}_2\text{AgInCl}_6$  DP nanocrystals at different pressures. (d) Chromaticity coordinates of the emissions. (e) Absorption spectra and (f) band gap of the  $\text{Cs}_2\text{AgInCl}_6$  DP nanocrystals at different pressures. The inset shows the direct band gap Tauc plots for the  $\text{Cs}_2\text{AgInCl}_6$  DP nanocrystals at 1 atm.

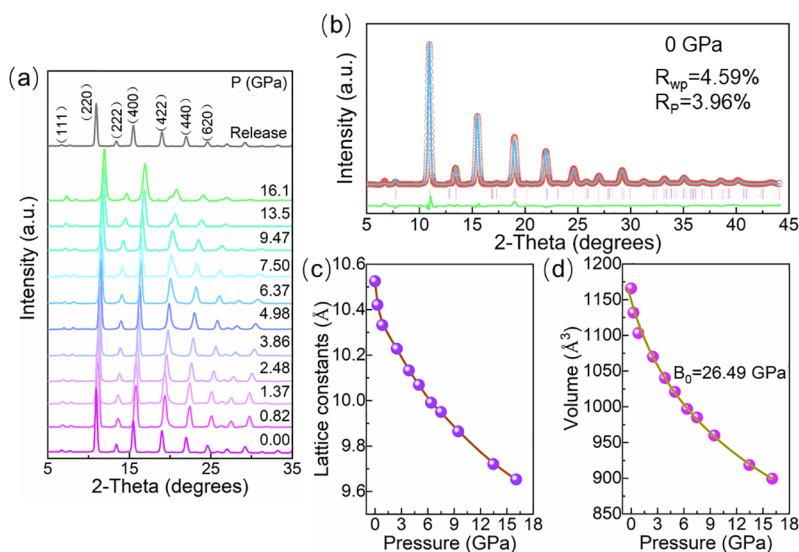


**Figure 3.** (a) Typical XRD patterns of the  $\text{Cs}_2\text{AgInCl}_6$  DP nanocrystals at different pressures. (b) Rietveld refinements of the XRD patterns obtained under ambient conditions. (c and d) Lattice constants and lattice volumes under high pressures.

The optical properties of the  $\text{Cs}_2\text{AgInCl}_6$  DP nanocrystals strongly depend on the response of the structure to compression. To explore the origin of the unusual optical evolution, we analyzed the synthesized  $\text{Cs}_2\text{AgInCl}_6$  DP nanocrystals via in situ high-pressure XRD. The representative XRD patterns for both compression and release to ambient conditions are shown in Figure 3a. Evidently, all of the Bragg diffraction peaks shift toward larger angles upon compression; however, no significant change occurs in the diffraction peak order, and accordingly, no phase transition occurs in the crystal structure. This Bragg diffraction peak shift is caused by the isotropic shrinkage of the unit cell under pressure. Figure 3b presents the Rietveld analysis profiles of the XRD data

obtained at ambient pressure. The fitted XRD pattern, obtained through Rietveld refinement, is in good agreement with that obtained experimentally. The Rietveld refinement indicates that the  $\text{Cs}_2\text{AgInCl}_6$  DP nanocrystals are in the cubic phase with space group  $Fm\bar{3}m$ , under ambient conditions. The changes in the lattice constant and cell volume are shown in panels c and d of Figure 3 and Table S2. The sample exhibits isotropic compressibility. In addition, the experimental pressure–volume ( $P$ – $V$ ) curves are fitted using the third-order Birch–Murnaghan equation of state (Figure 3d):



$$P = \frac{3}{2}B_0 \left[ \left( \frac{V_0}{V} \right)^{7/3} - \left( \frac{V_0}{V} \right)^{5/3} \right] \left\{ 1 + \frac{3}{4}(B_0' - 4) \left[ \left( \frac{V_0}{V} \right)^{3/2} - 1 \right] \right\}$$

where  $V_0$  is the volume at 0 GPa,  $B_0$  is the bulk modulus at 0 GPa, and  $B_0'$  is the derivative of the bulk modulus with respect to pressure. The cell volume decreases persistently with a bulk modulus of  $\sim 26.5$  GPa.

The underlying mechanisms of the pressure-induced anomalous emission are shown in Figure 4. On the basis of

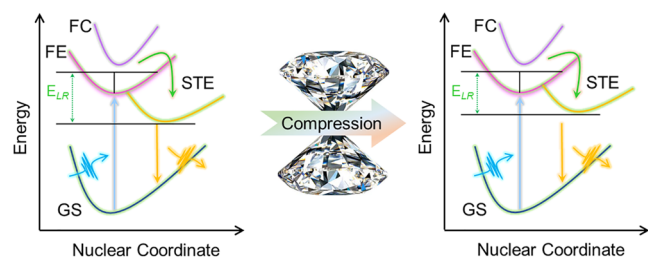


**Figure 4.** Schematic of the emission mechanism under ambient conditions and under pressure. Abbreviations: GS, ground state; FE, free exciton state; FC, free carrier state; STE, self-trapped exciton states;  $E_{LR}$ , lattice relaxation energy.

previously reported studies, the blue-shift of the emission can be mainly ascribed to the decreased lattice relaxation energy ( $E_{LR}$ ).<sup>21</sup> The contraction of the octahedron during the compression, decreased bond lengths, and unaltered Cl–In–Cl and Cl–Ag–Cl bond angles may also cause blue-shifts of the emission. The relationship between  $E_{LR}$  and the fwhm ( $\Delta$ ) can be expressed as  $\Delta \propto \sqrt{2E_{LR}K_B T}$ , where  $K_B$  represents the Boltzmann constant and  $T$  represents the temperature. This equation indicates that  $E_{LR}$  decreases with an increase in pressure on the  $\text{Cs}_2\text{AgInCl}_6$  DP nanocrystals.<sup>23,24</sup> Moreover, the remarkable decrease in the Stokes shift upon compression indicates a decrease in the electron–phonon coupling strength, as described above. The broad emission of the  $\text{Cs}_2\text{AgInCl}_6$  DP nanocrystals is mainly due to exciton self-trapping owing to the strong coupling between the exciton and the lattice. According to the XRD analysis, all of the octahedra exhibit persistent shrinkage under pressure, and it leads to a continuous cell contraction. The decreased emission intensity caused by the reduction in the exciton–phonon coupling strength may also result from the contraction of the octahedron during the compression. In the previously reported studies, this octahedral shrinking was found to increase the metal–halogen bond energy and reduce lattice deformations. Moreover, the shrinking of the octahedra increased the metal–halide orbital coupling and electronic band dispersion, causing a red-shift of the band gap of the  $\text{Cs}_2\text{AgInCl}_6$  DP nanocrystals. The octahedral shrinkage occurs synergistically with rotation and deformation during compression. The increase in the band gap observed at  $>5.81$  GPa may result from significant octahedral rotation and deformation. According to our comprehensive research, the octahedral shrinkage occurs synergistically with rotation and deformation during compression. The shrinking of the octahedra increased the metal halide orbital coupling and electronic band dispersion, reducing the band gap of the  $\text{Cs}_2\text{AgInCl}_6$  DP nanocrystals, while rotation and deformation of the octahedra can reduce the metal halide orbital coupling and reduce the valence band maximum, resulting in an increase in the band gap.

## CONCLUSION

In summary, we studied the structural–optical properties of  $\text{Cs}_2\text{AgInCl}_6$  DP nanocrystals upon compression at room temperature. The  $\text{Cs}_2\text{AgInCl}_6$  DP nanocrystals exhibited a direct band gap and broad emission, which can be attributed to exciton self-trapping due to strong electron–phonon coupling. Under hydrostatic pressure, the halide DP nanocrystals exhibited an abnormal blue-shift of the emission band accompanied by an absorption edge red-shift, which can be ascribed to the decreases in lattice relaxation energy. In addition, no phase transition occurred during pressurization. The findings of this study provide a platform for the development of an effective way to modulate and adjust the optical properties of halide DPs and demonstrate the necessity of improving their photovoltaic and optoelectronic performances via pressure engineering.

## ASSOCIATED CONTENT

### Supporting Information

The Supporting Information is available free of charge at <https://pubs.acs.org/doi/10.1021/acs.inorgchem.2c00185>.

Materials, description of the synthesis and in situ high-pressure experiments, fwhm of the PL spectra, details of chromaticity coordinates, and details of lattice constants and cell volumes (PDF)

## AUTHOR INFORMATION

### Corresponding Authors

**Quanjin Li** – State Key Laboratory of Superhard Materials, Jilin University, Changchun 130012, P. R. China; [orcid.org/0000-0002-4718-4156](https://orcid.org/0000-0002-4718-4156); Email: [liquanjun@jlu.edu.cn](mailto:liquanjun@jlu.edu.cn)

**Donglei Zhou** – State Key Laboratory of Superhard Materials, Jilin University, Changchun 130012, P. R. China; State Key Laboratory of Integrated Optoelectronics, College of Electronic Science and Engineering, Jilin University, Changchun 130012, P. R. China; [orcid.org/0000-0002-0664-0290](https://orcid.org/0000-0002-0664-0290); Email: [zhoudl@jlu.edu.cn](mailto:zhoudl@jlu.edu.cn)

### Authors

**Ao Chen** – State Key Laboratory of Superhard Materials, Jilin University, Changchun 130012, P. R. China; Changchun Institute of Optics, Fine Mechanics and Physics, Chinese Academy of Sciences, Changchun 130033, P. R. China

**Xiaoling Jing** – State Key Laboratory of Superhard Materials, Jilin University, Changchun 130012, P. R. China

**Tianyuan Wang** – State Key Laboratory of Integrated Optoelectronics, College of Electronic Science and Engineering, Jilin University, Changchun 130012, P. R. China

**Tingting Zhao** – State Key Laboratory of Superhard Materials, Jilin University, Changchun 130012, P. R. China

**Yu Zhang** – State Key Laboratory of Superhard Materials, Jilin University, Changchun 130012, P. R. China

**Rui Sun** – State Key Laboratory of Integrated Optoelectronics, College of Electronic Science and Engineering, Jilin University, Changchun 130012, P. R. China

**Xueting Zhang** – State Key Laboratory of Superhard Materials, Jilin University, Changchun 130012, P. R. China

**Ran Liu** – State Key Laboratory of Superhard Materials, Jilin University, Changchun 130012, P. R. China

**Bo Liu** – State Key Laboratory of Superhard Materials, Jilin University, Changchun 130012, P. R. China

Bingbing Liu – State Key Laboratory of Superhard Materials,  
Jilin University, Changchun 130012, P. R. China;  
orcid.org/0000-0003-3989-0891

Complete contact information is available at:  
<https://pubs.acs.org/10.1021/acs.inorgchem.2c00185>

### Author Contributions

<sup>†</sup>A.C. and X.J. contributed equally to this work.

### Notes

The authors declare no competing financial interest.

## ACKNOWLEDGMENTS

This work was financially supported by the National Key Research and Development Program of China (2018YFA0305900), the National Natural Science Foundation of China (11874172, U2032215, and 11634004), and the JLU Science and Technology Innovative Research Team (2017TD-01).

## REFERENCES

- (1) Boyd, C. C.; Cheacharoen, R.; Leijtens, T.; McGehee, M. D. Understanding Degradation Mechanisms and Improving Stability of Perovskite Photovoltaics. *Chem. Rev.* **2019**, *119* (5), 3418–3451.
- (2) Lin, D. X.; Shi, T. T.; Xie, H. P.; Wan, F.; Ren, X. X.; Liu, K.; Zhao, Y.; Ke, L. L.; Lin, Y.; Gao, Y. L.; Xu, X.; Xie, W. G.; Liu, P. Y.; Yuan, Y. B. Ion Migration Accelerated Reaction between Oxygen and Metal Halide Perovskites in Light and Its Suppression by Cesium Incorporation. *Adv. Energy Mater.* **2021**, *11* (8), 2002552.
- (3) Lan, S. G.; Li, W. C.; Wang, S.; Li, J. Z.; Wang, J.; Wang, H. Z.; Luo, H. M.; Li, D. H. Vapor-Phase Growth of CsPbBr<sub>3</sub> Microstructures for Highly Efficient Pure Green Light Emission. *Adv. Opt. Mater.* **2019**, *7* (2), 1801336.
- (4) Wei, J. H.; Liao, J. F.; Wang, X. D.; Zhou, L.; Jiang, Y.; Kuang, D. B. All-Inorganic Lead-Free Heterometallic Cs<sub>4</sub>MnBi<sub>2</sub>Cl<sub>12</sub> Perovskite Single Crystal with Highly Efficient Orange Emission. *Matter* **2020**, *3* (3), 892–903.
- (5) Zhou, L.; Xu, Y. F.; Chen, B. X.; Kuang, D. B.; Su, C. Y. Synthesis and Photocatalytic Application of Stable Lead-Free Cs<sub>2</sub>AgBiBr<sub>6</sub> Perovskite Nanocrystals. *Small* **2018**, *14* (11), 1703762.
- (6) Luo, J. J.; Wang, X. M.; Li, S. R.; Liu, J.; Guo, Y. M.; Niu, G. D.; Yao, L.; Fu, Y. H.; Gao, L.; Dong, Q. S.; Zhao, C. Y.; Leng, M. Y.; Ma, F. S.; Liang, W. X.; Wang, L. D.; Jin, S. Y.; Han, J. B.; Zhang, L. J.; Etheridge, J.; Wang, J. B.; Yan, Y. F.; Sargent, E. H.; Tang, J. Efficient and stable emission of warm-white light from lead-free halide double perovskites. *Nature* **2018**, *563* (7732), 541–545.
- (7) Slavney, A. H.; Hu, T.; Lindenberg, A. M.; Karunadasa, H. I. A Bismuth-Halide Double Perovskite with Long Carrier Recombination Lifetime for Photovoltaic Applications. *J. Am. Chem. Soc.* **2016**, *138* (7), 2138–2141.
- (8) Filip, M. R.; Hillman, S.; Haghighirad, A. A.; Snaith, H. J.; Giustino, F. Band Gaps of the Lead-Free Halide Double Perovskites Cs<sub>2</sub>BiAgCl<sub>6</sub> and Cs<sub>2</sub>BiAgBr<sub>6</sub> from Theory and Experiment. *J. Phys. Chem. Lett.* **2016**, *7* (13), 2579–2585.
- (9) Volonakis, G.; Haghighirad, A. A.; Milot, R. L.; Sio, W. H.; Filip, M. R.; Wenger, B.; Johnston, M. B.; Herz, L. M.; Snaith, H. J.; Giustino, F. Cs<sub>2</sub>InAgCl<sub>6</sub>: A New Lead-Free Halide Double Perovskite with Direct Band Gap. *J. Phys. Chem. Lett.* **2017**, *8* (4), 772–778.
- (10) Lee, W.; Hong, S.; Kim, S. Colloidal Synthesis of Lead-Free Silver–Indium Double-Perovskite Cs<sub>2</sub>AgInCl<sub>6</sub> Nanocrystals and Their Doping with Lanthanide Ions. *J. Phys. Chem. C* **2019**, *123* (4), 2665–2672.
- (11) Arfin, H.; Kaur, J.; Sheikh, T.; Chakraborty, S.; Nag, A. Bi(3+)–Er(3+) and Bi(3+)–Yb(3+) Codoped Cs<sub>2</sub>AgInCl<sub>6</sub> Double Perovskite Near-Infrared Emitters. *Angew. Chem., Int. Ed. Engl.* **2020**, *59* (28), 11307–11311.
- (12) Liu, Y.; Molokeev, M. S.; Xia, Z. Lattice Doping of Lanthanide Ions in Cs<sub>2</sub>AgInCl<sub>6</sub> Nanocrystals Enabling Tunable Photoluminescence. *Energy Material Advances* **2021**, *2021*, 1–9.
- (13) Li, S.; Hu, Q.; Luo, J.; Jin, T.; Liu, J.; Li, J.; Tan, Z.; Han, Y.; Zheng, Z.; Zhai, T.; Song, H.; Gao, L.; Niu, G.; Tang, J. Self-Trapped Exciton to Dopant Energy Transfer in Rare Earth Doped Lead-Free Double Perovskite. *Adv. Opt. Mater.* **2019**, *7* (23), 1901098.
- (14) Atuchin, V. V.; Beisel, N. F.; Galashov, E. N.; Mandrik, E. M.; Molokeev, M. S.; Yeliseyev, A. P.; Yusuf, A. A.; Xia, Z. G. Pressure-Stimulated Synthesis and Luminescence Properties of Microcrystalline (Lu, Y)(3)AlSiO<sub>12</sub>:Ce<sup>3+</sup> Garnet Phosphors. *ACS Appl. Mater. Interfaces* **2015**, *7* (47), 26235–26243.
- (15) Zhuravlev, Y. N.; Atuchin, V. V. First-Principle Studies of the Vibrational Properties of Carbonates under Pressure. *Sensors* **2021**, *21* (11), 3644.
- (16) Li, Q.; Wang, Y. G.; Pan, W. C.; Yang, W. G.; Zou, B.; Tang, J.; Quan, Z. W. High-Pressure Band-Gap Engineering in Lead-Free Cs<sub>2</sub>AgBiBr<sub>6</sub> Double Perovskite. *Angew. Chem.-Int. Ed.* **2017**, *56* (50), 15969–15973.
- (17) Li, N. N.; Zhang, Q.; Wang, Y. G.; Yang, W. G. Perspective on the pressure-driven evolution of the lattice and electronic structure in perovskite and double perovskite. *Appl. Phys. Lett.* **2020**, *117* (8), 080502.
- (18) Lim, S. C.; Lin, H. P.; Tsai, W. L.; Lin, H. W.; Hsu, Y. T.; Tuan, H. Y. Binary halide, ternary perovskite-like, and perovskite-derivative nanostructures: hot injection synthesis and optical and photocatalytic properties. *Nanoscale* **2017**, *9* (11), 3747–3751.
- (19) Tran, T. T.; Panella, J. R.; Chamorro, J. R.; Morey, J. R.; McQueen, T. M. Designing indirect-direct bandgap transitions in double perovskites. *Mater. Horizons* **2017**, *4* (4), 688–693.
- (20) Ma, Z.; Li, Q.; Luo, J.; Li, S.; Sui, L.; Zhao, D.; Yuan, K.; Xiao, G.; Tang, J.; Quan, Z.; Zou, B. Pressure-Driven Reverse Intersystem Crossing: New Path toward Bright Deep-Blue Emission of Lead-Free Halide Double Perovskites. *J. Am. Chem. Soc.* **2021**, *143* (37), 15176–15184.
- (21) Zhang, L.; Fang, Y.; Sui, L.; Yan, J.; Wang, K.; Yuan, K.; Mao, W. L.; Zou, B. Tuning Emission and Electron–Phonon Coupling in Lead-Free Halide Double Perovskite Cs<sub>2</sub>AgBiCl<sub>6</sub> under Pressure. *ACS Energy Lett.* **2019**, *4* (12), 2975–2982.
- (22) Liu, G.; Kong, L. P.; Gong, J.; Yang, W. G.; Mao, H. K.; Hu, Q. Y.; Liu, Z. X.; Schaller, R. D.; Zhang, D. Z.; Xu, T. Pressure-Induced Bandgap Optimization in Lead-Based Perovskites with Prolonged Carrier Lifetime and Ambient Retainability. *Adv. Funct. Mater.* **2017**, *27* (3), 1604208.
- (23) Saitoh, A.; Komatsu, T.; Karasawa, T. Exciton-phonon interaction and conversion of excitons from free to self-trapped states in layered metal iodide crystals under hydrostatic pressure. *J. Lumin.* **2000**, *87–89*, 633–635.
- (24) Tsujimoto; Nishimura; Nakayama. Hydrostatic pressure effects on the free and self-trapped exciton states in CsI. *Physical review. B, Condensed matter* **1996**, *54* (23), 16579–16584.